Fermilab

FERMILAB-Pub-01/050 May 2001

Calibration of Saturated Liquid Helium Weir Flowmeter at Fermilab

M.W. McGee, D.M. France* and R.C. Sanders

Fermi National Accelerator Laboratory, Batavia, Illinois 60510†
Department of Mechanical Engineering, University of Illinois at Chicago, Chicago, IL. 60607*

The flow of saturated liquid helium at 4.2 K was studied in a unique weir flowmeter mounted inside a duct. The objective was to develop a calibration for helium flow rate in the weir, and thereby, making it a viable flowmeter. The weir flowmeter was tested in a liquid helium system at Fermi National Accelerator Laboratory used for cooling the superconducting magnets in the experimental areas of the site. Unlike for open channel weir devices, the calibration of this flowmeter was influenced by both the liquid flow thru the weir notch and the vapor flow over it. The results of this study and the calibration are presented taking into account effects of both liquid and vapor.

Keywords: two-phase helium flow; weir flowmeter; liquid helium

Nomenclature

English symbols

C_d Coefficient of discharge [dimensionless]
DP Measured pressure drop [MPa]
f Pressure drop with density term [MPa(100)cc/g]
g Acceleration due to gravity [m/s^2]
h Weir level, measured height of liquid surface from bottom of liquid level probe [cm]
h_o Level of bottom of V-notch measured from bottom of liquid level probe [cm]
K Parameter [cm$^{0.5}$/s]
P_I Pressure at point i [MPa]
P Measured pressure [MPa]
Q_a Predicted flow rate case (13a) [l/hr]
Q_b Predicted flow rate case (13b) [l/hr]
Q_c Predicted flow rate case (13c) [l/hr]
Q_d Predicted flow rate case (13d) [l/hr]
Q_{th} Theoretical liquid volumetric flow rate [l/hr]
$V_{Bl}(\eta)$ Liquid velocity as a function of level at B [m/s]
$w(\eta)$ Width of weir V-notch as a function of level [cm]

Greek symbols

Δ_v Vapor pressure drop across the weir plate [MPa]
θ Angle of v-notch [°]
ρ_l Liquid density [g/cc(100)]
ρ_v Vapor density [g/cc(100)]
η Level above bottom of liquid level probe [cm]

Introduction

Flow measurement devices for single and two-phase flow take on a variety of forms. In this investigation, a weir (commonly used for open channel single-phase liquid flow) was used to measure the flow of liquid helium in a two-phase mixture of liquid and vapor. For two thousand years, weirs have been used to raise and divert water flow in channels. The formal study of weir flowmeters in open channels has occurred over the last 250 years[1]. The design of the helium weir is presented along with the development of a calibration technique. The results are a reliable flowmeter for an important but difficult cryogenic application.

The goal of this study was to develop and verify an accurate calibration for a weir flowmeter for liquid helium in a two-phase mixture. The immediate application is in support of superconducting magnets used to steer high energy proton beams at Fermi National Accelerator Laboratory. These magnets make up a circular accelerator called the Tevatron (a 900 GeV proton-antiproton collider)[2]. The weir flowmeter was developed to provide accurate flow measurement for helium systems at Fermilab, however, the results are generally applicable to measurement of liquid helium flow.

† Work supported by the US Department of Energy under contract number DE-AC02-76CHO3000.

Method

In the upper portion of the weir flow device, there is a continuous helium vapor flow region generated by evaporation in the system. Unlike weirs used for water flow in open channels, the liquid helium weir flow is influenced by the vapor phase as well as the liquid phase. Experimentation has since confirmed that the two-phase helium flow within the Tevatron is most probably entirely in the stratified flow regime[2,3].

When two-phase helium flow is stratified, the liquid flows in the bottom of the tube, and each phase travels at a different average velocity (non-homogenous flow), where the vapor velocity and the interfacial shear stress are low[4]. The measurement of the liquid flow rate in this flow regime accounts for nearly the entire helium flow rate.

Currently, there are several ways to measure the liquid component of a two-phase helium flow. Each existing method involves controlled conditions which lead to either large or elaborate devices and which are very expensive. Flow measurement is obtained through either mass flow or volumetric flow, and knowledge of fluid density (two-phase average density) is required for direct conversion between the two[5].

Weir Theory

Often used in an open channel, a weir restricts fluid flow forming a barrier. The crest of a weir refers to the edge of the plate or surface of the flowing fluid as shown in Figure 1. A sheet of fluid stemming from this crest is called the nappe. Free discharge occurs when the nappe discharges into gas or vapor. The discharge is said to be submerged or drowned when (as in Figure 1(b)) it is partially beneath the exit channel fluid[6]. A sharp-crested weir, having a sharp upstream corner or edge from which the fluid flows, invokes a condition where the fluid may spring clear (free discharge) of the plate on the downstream side[1,7].

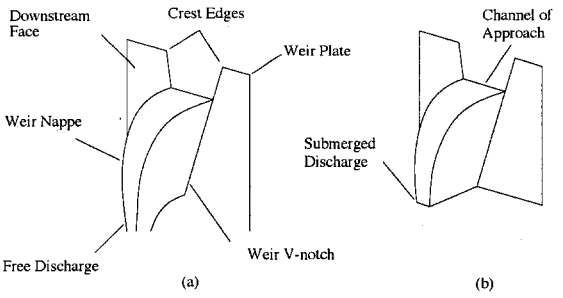

Figure 1 Diagram of a V-notch weir.

Nappe aeration (ventilation to gas or vapor) of a full-width horizontal weir is necessary to prevent liquid from being drawn inward (entrainment). In this case, discharge will increase as a result of the low-pressure region at a particular head (the vertical distance from the crest to the liquid surface upstream). When not enclosed, a partial channel span of the fluid causes automatic aeration[8]. Nappe contraction occurs at the top of the weir due to gravity and the conversion of potential to kinetic energy. Contraction at the bottom is the result of the vertical velocity component of the inner weir face[7].

Total aeration implies that the lower nappe surface is completely ventilated. When side ventilation of the nappe is restricted, a partial vacuum will result due to the removal of gas or vapor by the overflowing jet. This partial vacuum will increase discharge and induce fluctuations, influencing the nappe shape[6]. In general, aeration problems lead to unsteady conditions causing decreased accuracy and resolution of the flow device[6,7].

The V-notch weir incurs an additional stream contraction due to the crest's sharp vertical edges. Lower flow rates for V-notch weirs are recommended and repeatability requires that sharp edges be maintained[6,8]. There is a tendency for the nappe of a rectangular weir to adhere (cling) to the downstream face of the weir plate at low head pressures. The use of a V-notch plate reduces this effect, increasing accuracy at low heads and increasing rangability[6,7,9]. At low head, surface tension affects the discharge and can cause the nappe to adhere to the weir blade or upstream face of the plate thus affecting the nappe shape[7].

Fermilab Weir Design

The weir flowmeter (Figure 2) installed in September 1992 at the Proton Service Building #1 (PS1) was constructed from (AISI 304) stainless steel, designed to withstand an internal pressure of 11.2 MPa (gauge pressure), while externally surrounded by vacuum. The flowmeter inner vessel and vacuum shell were fabricated using a standard 10.16 cm and 15.24 cm stainless steel pipe tee, respectively. Two pressure taps located at the liquid base of the throat and exit of the flowmeter allow for important pressure-drop measurements. Dimensions of the weir vessel and shell are shown in Figure 2.

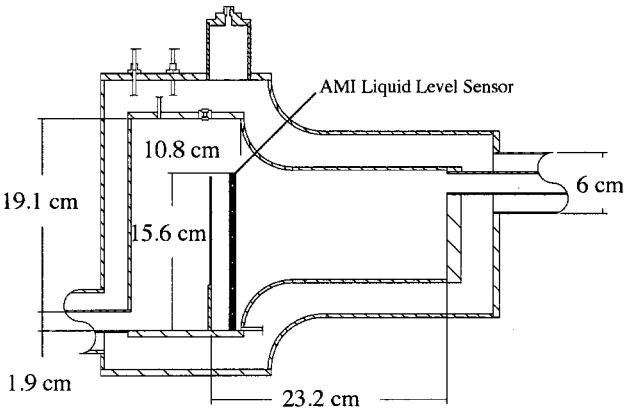

Figure 2 Diagram of enclosed liquid helium weir flowmeter at PS1 (Fermilab).

Weir Plate

The stainless steel plate shown in Figure 3 is 15.24 (± 0.038) cm high, 7.62 (± 0.038) cm in width, and 0.3175 (± 0.089) cm thick. The level to the bottom of the V-notch (h_o) is 5.08 cm. A 4° (± 0° 15') angle was cut into the sharp-crested V-notch weir plate by an electrodischarge machining (EDM) process using a 0.254 mm diameter wire. A thin sharp edge was established by milling a slot and then grinding the upstream surface flat to within ± 0.127 mm.

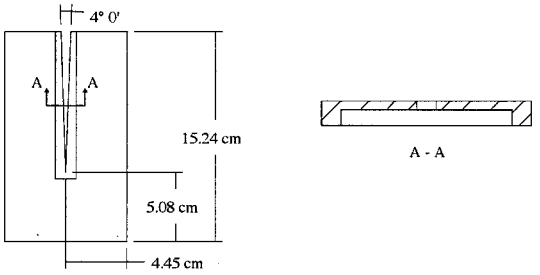

Figure 3 Weir plate and discharge.

Flow Description

The stratified two-phase helium flow (Figure 4) entering the vessel has separated phases with vapor at the top and the liquid flowing beneath. The space above the weir is sized to prevent excessive pressure drop in the vapor flow. On the downstream side of the weir, the vapor and the liquid exit the vessel together[10].

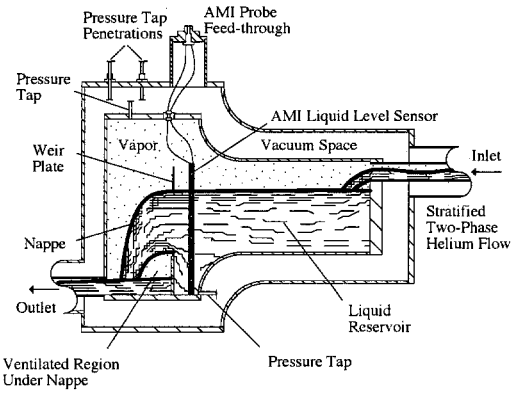

Figure 4 Weir flowmeter.

In order to promote free discharge of the nappe, the weir was sharp crested with the discharge well below the V-notch. A slight decrease in level of liquid helium near the weir plate is due to contraction, which is imposed by the edges of the crest[12]. The normal operating pressure within the flowmeter is 0.138 MPa and the measured liquid flow rate range is between 5.76 and 197 l/hr.

Flow measurement repeatability is dependent on the free discharge of the nappe. Other factors affecting the free discharge include the space necessary to adequately ventilate or equalize pressure surrounding the nappe, and the condition when the discharge flow is submersed by liquid within the exit channel. The design level (h_o) helps to prevent this condition. A favorable characteristic of liquid helium, which possesses a surface tension over one hundred times greater than water, is that it is unlikely to cling to the plate's surface[10].

Theoretical Relations

To derive a theoretical equation for liquid flow through a V-notch weir, apply Bernoulli's equation to the liquid flow path between points A and B in Figure 5. Point A is on the liquid surface of the reservoir at level $\eta = h$, and is far enough behind the weir plate so that the liquid velocity is negligible. Point B is in the plane of the weir plate notch at level η, $h_o < \eta < h$, in the flowing liquid:

$$\frac{P_A}{\rho_l} + h = \frac{P_B(\eta)}{\rho_l} + \frac{\left(V_{Bl}(\eta)\right)^2}{2g} + \eta \qquad (1)$$

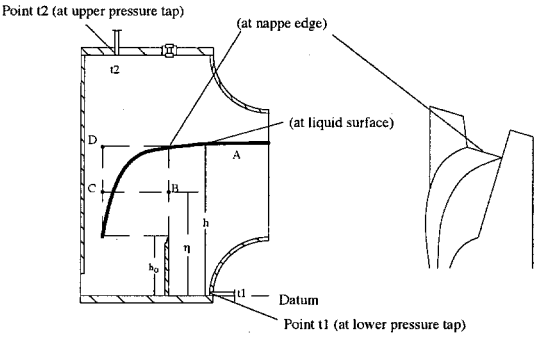

Figure 5 Diagram defining points within flowmeter.

In Figure 5, point C is located in the downstream vapor at the same level η as point B, and point D is located in the downstream vapor at the same level h as point A. Assume the pressures at points B and C to be equal and apply Bernoulli's equation to the vapor flow path between points C and D ignoring frictional losses and changes in vapor velocity between those two points.

$$P_B(\eta) = P_C(\eta) = P_D + \rho_v(h - \eta) \qquad (2)$$

Define the vapor pressure drop across the weir plate Δ_v as:

$$\Delta_v = P_A - P_D \qquad (3)$$

Solving for the liquid velocity at point B:

$$V_{Bl}(\eta) = \sqrt{\left(\frac{2g(\rho_l - \rho_v)}{\rho_l}\right)\left((h - \eta) + \frac{\Delta_v}{(\rho_l - \rho_v)}\right)} \qquad (4)$$

The flow rate through any weir is determined by integration of the form

$$Q_{th} = C_d \int_{h_0}^{h} V_{Bl} w(\eta) d\eta \qquad (5)$$

Where $0 \le C_d \le 1$ is an experimentally determined coefficient that takes into account the affects of non-ideal

liquid flow. A nondimensional correlation (developed by Lenz)[12] predicts a 0.6 discharge coefficient for the liquid helium flowmeter at Fermilab. The V-notch width as a function of level is:

$$w(\eta) = 2(\eta - h_0)\tan(\theta/2) \quad (6)$$

The volumetric liquid flow rate through a V-notch weir is then:

$$Q_{th} = K\int_{h_0}^{h}\sqrt{h-\eta+\Delta_v}\,(h-h_0)\,d\eta \quad (7)$$

Parameter K is defined as

$$K = 2C_d\tan(\theta/2)\sqrt{\frac{2g(\rho_l-\rho_v)}{\rho_l}} \quad (8)$$

Evaluating the integral produces

$$Q_{th} = K\left[\frac{4}{15}(h-h_0+f)^{5/2} - \frac{4}{15}f^{5/2} - \frac{2}{3}(h-h_0)f^{3/2}\right] \quad (9)$$

Where f is defined as

$$f = \frac{\Delta_v}{\rho_l - \rho_v} \quad (10)$$

If the vapor pressure drop is negligible, $\Delta_v = 0$, such as is in open channel flow then

$$Q_{th} = \frac{8}{15}C_d\tan(\theta/2)\sqrt{\frac{2g(\rho_l-\rho_v)}{\rho_l}}h^{5/2} \quad (11)$$

The small enclosed design of the weir flowmeter in this study creates a restriction of the vapor flow path causing frictional losses which affect vapor pressure. The vapor pressure drop, Δ_v, is increased, which is not considered in Equations (2) and (11), resulting in an acceleration of the liquid across the weir plate. Such a pressure change under normal operating conditions may decrease the liquid level from 2 mm to 4 mm. The pressure taps in the Fermilab flowmeter were installed as an alternative means to measure weir level, therefore, pressure tap placement was not chosen to be accurate. Given the circumstances, Equation (9) should not be used to calculate flow rate, because of the lack of vapor pressure drop Δ_v accuracy.

If the vapor density ρ_v, is set equal to 0, then Equation (9) becomes the theoretical equation[12] (Lenz from Equation (2)) commonly used for open channel V-notch weirs with a dense liquid such as water in an air atmosphere:

$$Q_{th} = \frac{8}{15}C_d\tan(\theta/2)\sqrt{2g}\,h^{5/2} \quad (12)$$

The two phase helium in the Fermilab weir has a vapor density about 10% that of the liquid; so that the effects of the vapor density cannot be ignored. In general, Equation (12) should not be used when the fluid is liquid helium.

Experimental Apparatus

The PS1 liquid helium dewar has a 400 l capacity (with an inner radius of 37.62 cm), it receives two-phase return flow from the magnet string. Saturated vapor returns to the cold end (shell side) of the heat exchanger.

During operation, the dewar is maintained at 70% of its capacity. The conversion of 5.3 l per percent is applied between the capacity range of 10% to 80%. An American Magnetics Inc. (AMI) liquid level sensor for helium is suspended a lateral distance of 2.20 cm from the weir plate. The sensor is 15.56 cm long and 6.35 cm in diameter. Level measurements are possible only over its active length of 14.61 cm. The AMI liquid level sensor is superconducting (made of Nb-Ti alloy) and provides continuous linear indication of level with an output signal of 0.22 volts per cm at 50 mA[11].

The surface wake created by slug flow of liquid helium entering the weir reservoir does have a small effect on the AMI level measurement accuracy. The results of a statistical analysis of the weir level data showed a maximum standard deviation of 1.55 mm, which is within the resolution of the device.

The two capillary tubes (pressure taps) stemming from the weir inner vessel (Figure 5) are connected to an ITT Barton differential pressure transducer Model 6001. This differential pressure transducer operates over a range of 0 to 995 Pa, with an accuracy of 0.2% and a maximum working pressure of 1.03 MPa. A Setra Systems Model 205-2 pressure transducer is connected to the inner vessel of the dewar using a separate capillary tube.

The bottom pressure tap sensing line is small in diameter (3.2 mm) with a thickness of 0.889 mm. This tube formed in a helical spiral with a very gradual incline, used to minimize vertical distance between the warm and cold end. The maximum measured standard deviation of the differential pressure was 154 Pa, which was considered over the 45 data points. Including the differential pressure measurement in the flow rate estimation helped to account for the discrepancies in the data.

Calibration Tests

The volumetric flow rate across the weir plate was measured using a liquid helium dewar near the weir flowmeter outlet. The flow rate was based on a change in volume of liquid within the dewar over time. A test started from full operation level of the dewar (70%). Flow entered from the weir flowmeter, and at the same time an electric heater was used to boil off helium. The next effect was a gradual reduction in level of the dewar to 50%. At this point, the heater was turned off, and the dewar was allowed to fill back to 70%. Then the cycle was repeated. Dewar levels were recorded as data in both the boil-off and dewar fill legs of the cycle. This range of dewar level was selected to provide a sufficient calibration period while observing system operational limits.

During the boil-off portion of the cycle, a heater controller accurately reduced the liquid helium level at different rates using an electric heater centrally mounted, near the bottom of the dewar. Dewar heater test values ranged from 30 to 130 W. The liquid helium dewar and weir flowmeter test setup at PS1 are shown in Figure 6.

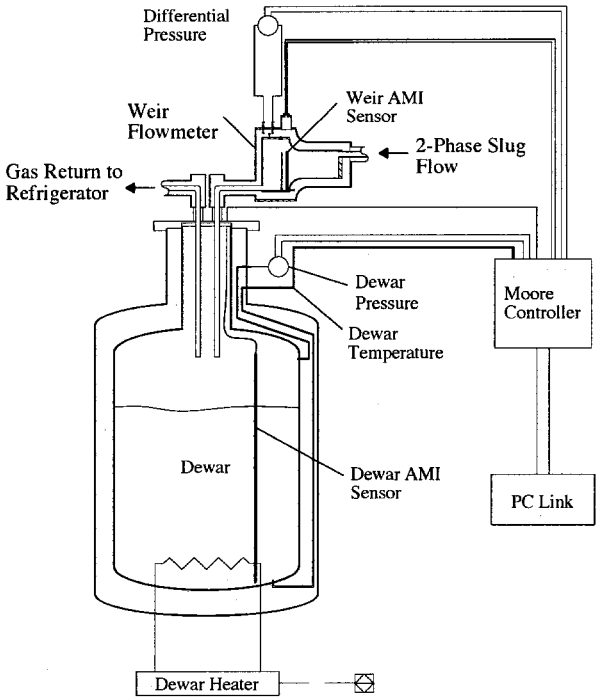

Figure 6 PS1 weir flowmeter and dewar calibration test set-up.

Results

During a test, measurements were made of weir level, weir differential pressure and dewar pressure. Each data point was the average of 500 to 1740 measurements. During data acquisition, the Moore controller retrieved a dewar level value every 10 seconds. An Excel spreadsheet calculated each flow rate data point using the slope, or the averaged rate of change of dewar level over time and dewar cross-sectional area. The boil-off contribution was calculated using the averaged heater power, liquid helium density and the latent heat of vaporization. The helium properties were found using a Visual Basic program with two state conditions, dewar pressure and temperature (assumed to be identical to the weir vessel conditions).

Selection of appropriate data from the fill and boil test legs began with plotting dewar and weir level as a function of time, as shown in Figure 7. The increasing or decreasing slope of the dewar level was inspected for non-uniformity and the weir level for large fluctuations. Applying these criteria, a section of continuous measurements was chosen for the data reduction. Such a section is shown between the vertical lines in Figure 7 at 0.3 and 3.7 hours. The criteria were put into numerical form using a standard deviation of 1.524 mm for weir level, 153.8 Pa for weir differential pressure and 441.3 Pa for dewar pressure. In order to be selected, this continuous group of data needed a minimum number of data points based on the slope of the dewar level as a function of time.

Forty five tests met the selection criteria and were processed for flow rate determination. The calculation of flow rate within the Excel spread sheet was completed by using the weir level, dewar level, heater power and time difference. The calculation of helium properties followed and finally, the boil-off.

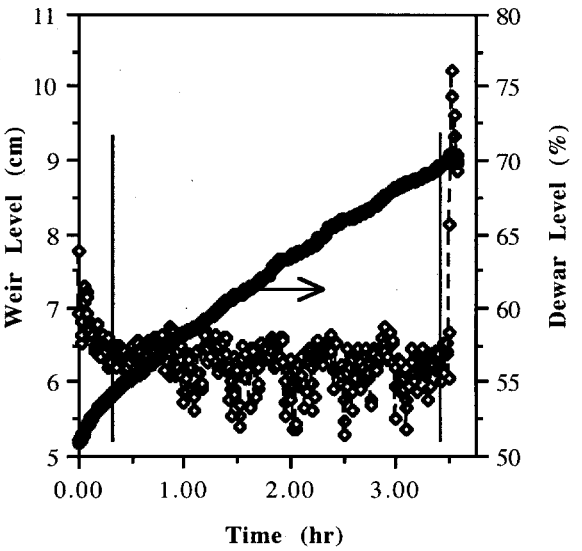

Figure 7 Data measurements.

Calibration Curve

Data from the 45 weir flow rate tests were used to develop a calibration equation using a FORTRAN code that minimized the sum of the errors squared. Table 1 presents the four calibration equations for the measured flow rate data with the best accuracy from Equation (13c). The final predictive forms shown in Table 1 were the result of a systematic elimination, where the acceptance criteria was based on convergence and best fit.

Table 1. Summary of optimum prediction forms.

Eqn.	Form
13a	$Q_a = 7.488x10^{-10}(h + 47.94DP + 0.266P + 1.655)^{7.625}$
13b	$Q_b = (0.1075h + 112.9DP - 47.26)^{1.738}$
13c	$Q_c = (0.0001h + 84.69DP + 1.053P - 37.43)^{1.897}$
13d	$Q_d = (0.0311DP)^{8.626}$

Figure 8, depicts the comparison between the flow rate data and each equation in Table 1 as a function of weir level. Figure 9, shows the "best fit" comparison of predicted case (13c) and the flow rate data.

Data Error and Accuracy

The scatter plot of the original theoretical equation, Equation (11) Figure 10, has systematic errors and overpredicts the data in the negative direction. A series of scatter plots for both theoretical flow rates and each of the predicted flow rates are shown in Figures 11 through 15. The associated root mean squared (RMS) error value for this case is 22.4%. When the effect of the vapor velocity is included, as shown in the corrected theoretical equation scatter plot, Figure 11 the error band is ±20% and the RMS value is reduced to 14%. The predicted cases (13a)

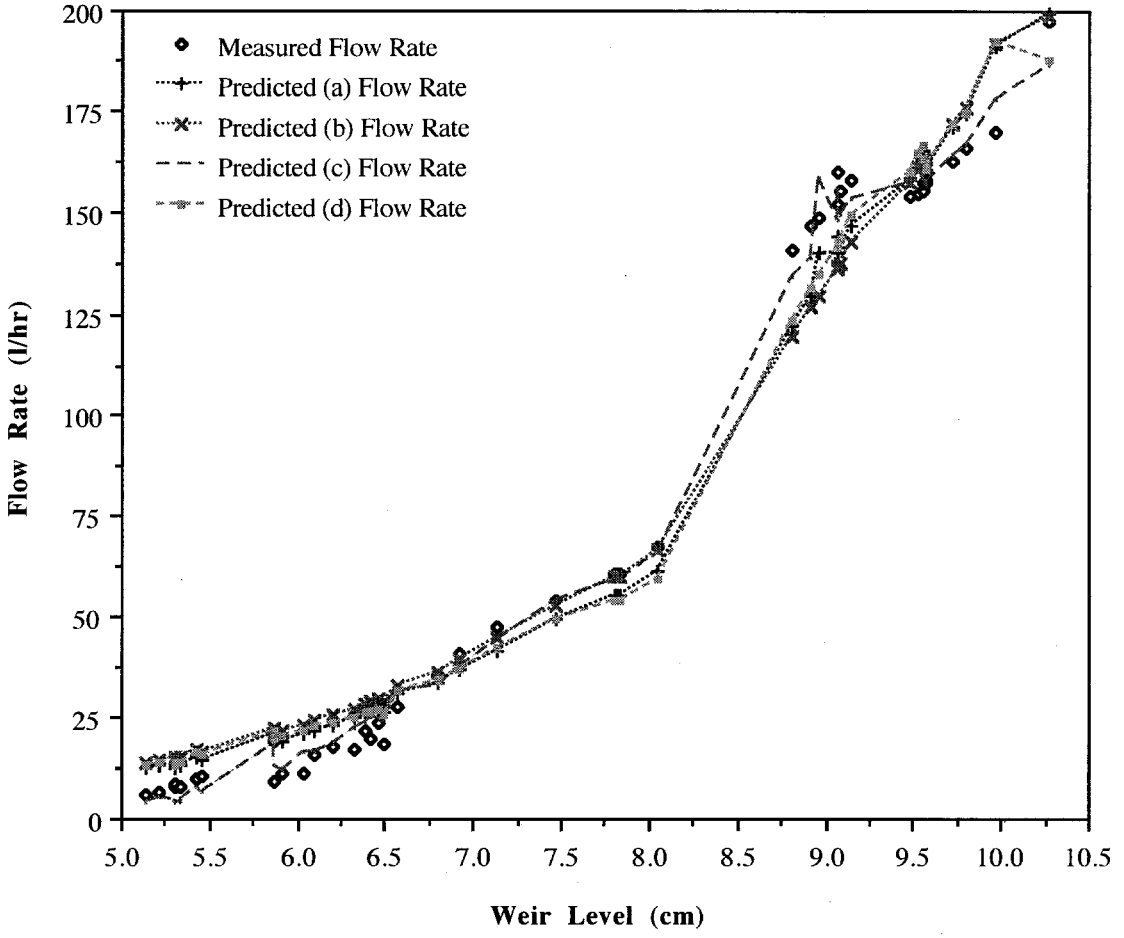

Figure 8 Comparison of measured flow rate and predicted cases (13a-13d) from Table 1 as a function of weir level.

and (13b) shown in Figures 12 and 13 display better accuracy with RMS values of 27.7% and 14.5%, respectively. The predicted case (13c) in Figure 14 is the most accurate form with an associated RMS value of 13.8%. Finally, the simple form that only considers differential pressure (Figure 15) has a moderate RMS value of 30.5%.

Discussion

Comparing calibration Equations (13a) and (13b) in Figures 12 and 13, it is seen that the omission of static pressure in Equation (13b) was not detrimental to the prediction accuracy. This result indicates the major importance of the differential pressure compared to the static pressure. Using a different form Equation (13a) was recast including the static pressure produce the most accurate of the calibration equations as seen in Figure 14. However, Equation (13b) predicted the data reasonably well and, with one less variable, it is easier to apply than the slightly more accurate Equation (13c).

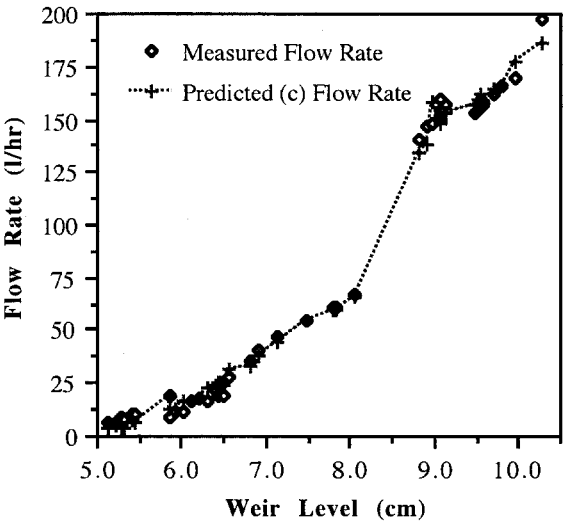

Figure 9 Comparison of measured flow rate and the correlation form case (13c) from Table 1 as a function of weir level.

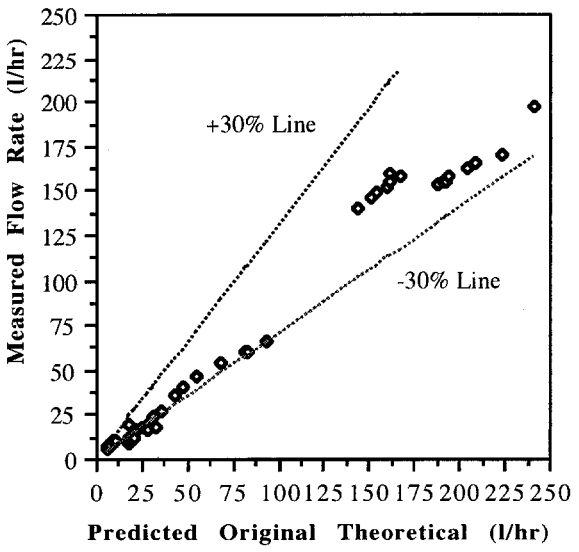

Figure 10 Scatter plot of original theoretical flow rate from Equation (11) versus experimentally measured flow rate.

In the enclosed weir of this study, the vapor flow rate can be substantial and can affect the liquid flow rate. To accurately account for this effect, a measurement of weir differential pressure was necessary. In addition, measurement of weir pressure is related to the driving force of liquid through the weir. Both parameters were included in Equation (13c), which is the best prediction of the data. The results of Figure 9 show the prediction of Equation (13c) compared to the measurements using only weir height as a parameter. The predictions are good. It should be noted that the curve is not smooth because the effect of pressure is not shown.

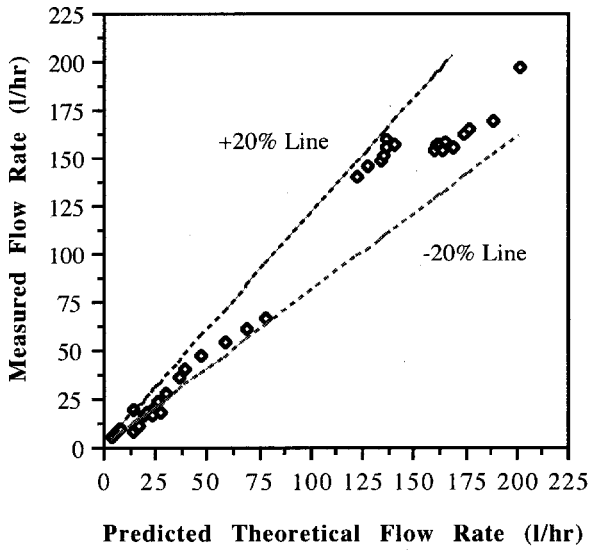

Figure 11 Scatter plot of predicted theoretical flow rate with vapor correction, from Equation (11) versus experimentally measured flow rate.

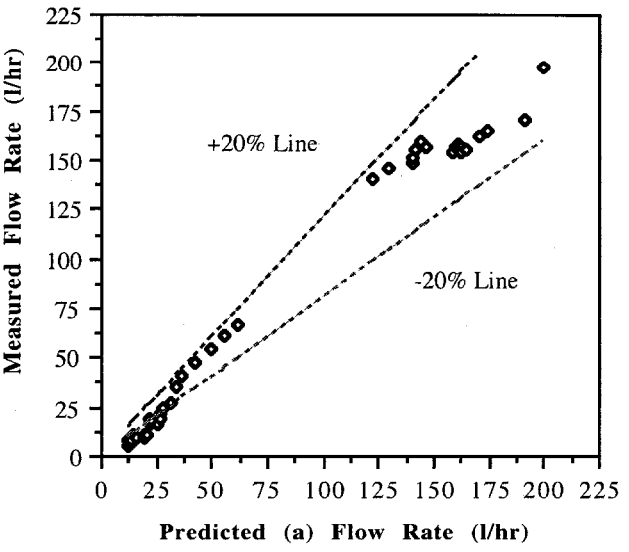

Figure 12 Scatter plot of predicted case 13a (Equation (13a) in Table 1) flow rate versus experimentally measured flow rate.

It is important to point out the small value of the constant in front of the weir level term in Equation (13c), which might imply that correlation of the calibration data is mostly due to the weir differential pressure. However, the lower pressure tap was placed at the bottom of the reservoir, so this measurement also includes the liquid head or level. Predictive forms with weir level alone were considered. These forms could not adequately describe the flow rate over the entire range. Equation (13d) provides the simplest prediction form based only on weir differential pressure with weir level included in this pressure measurement. The accuracy is good showing that the system pressure has little effect on the flow rate

In view of the importance of vapor velocity effects on liquid helium flow in the weir, it is not surprising that the original theoretical flow Equation (11) did not predict the data as well as Equations (13a) – (13d). Equation (11) does not account for vapor velocity using differential pressure or any other parameter. Add the differential pressure to Equation (11) yielded Equation (9), and the data prediction was improved to the same order as Equations (13a) and (13d). However, including the variables of weir level, weir differential pressure and static pressure in the from of Equation (13c) produced the best results with most the data falling within 10% error bounds. (Note that the weir level comes into the equation both as a distinct variable and as part of the differential pressure measurement.)

Looking at Figures (10) – (15), it is seen that all equations involved inaccuracies at very low flow rates. In this regard, the data were scrutinized using the discharge coefficient as a parameter. The measured discharge coefficient using Equation (14)

$$C_d = \frac{Q}{Q_{th}} \tag{14}$$

is shown in Figure 16.

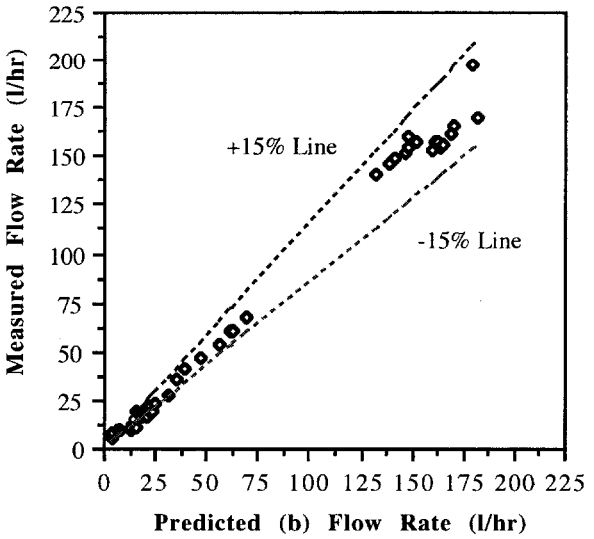

Figure 13 Scatter plot of predicted case 13b (Equation (13b) in Table 1) flow rate versus experimentally measured flow rate.

The measured discharge coefficients show a somewhat inconsistent trend. This situation is explained as follows. Starting with the circled data in Figure 16, representing the low flow region, it was determined that the liquid level in the weir was barely above the bottom of the V-notch. Under such conditions, liquid is known to cling to the face of the weir plate, which acts to decrease flow resistance. The resulting high discharge coefficient measured in this region are consistent with such an occurrence, and these data should not be expected to be equally well predictable by equations dominated by data from free discharge flow.

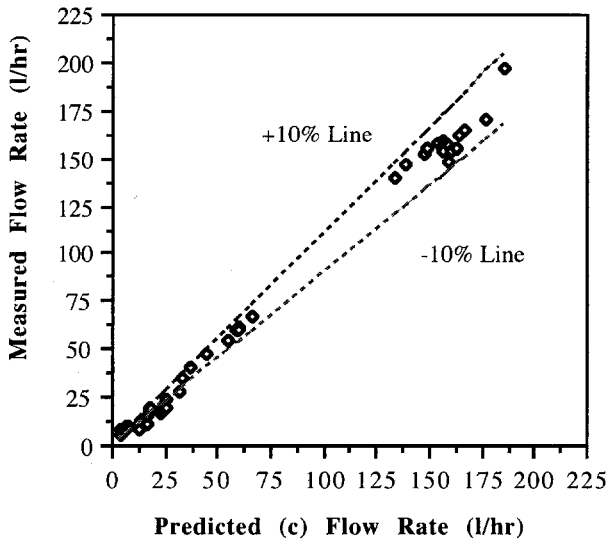

Figure 14 Scatter plot of predicted case 13c (Equation (13c) in Table 1) flow rate versus experimentally measured flow rate.

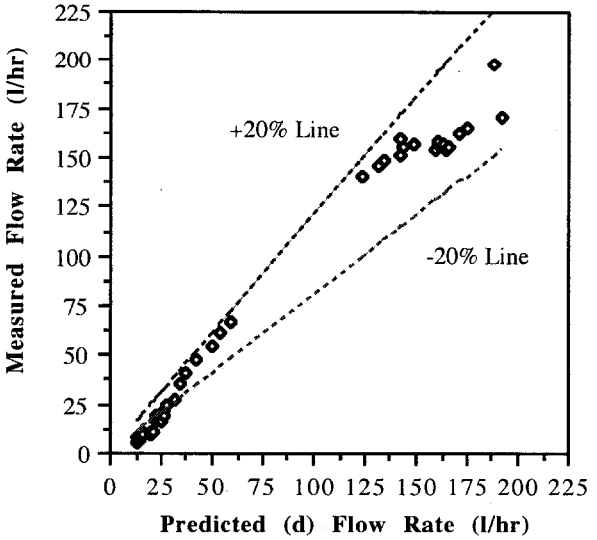

Figure 15 Scatter plot of predicted case 13d (Equation (13d) in Table 1) flow rate versus experimentally measured flow rate.

At weir levels slightly higher than the circled data (wall clinging effect) in Figure 16, the discharge coefficient is seen to drop significantly and abruptly. The abruptness points to the discharge coefficient beginning to move from the weir plate into a semi-free discharge. In this regime, there is some flow along the plate and the intermittent nature leads to higher flow resistance and low discharge coefficients. Eventually, at weir levels above about 6.6 cm, the measured discharge coefficients reach a more consistent trend. (With some scatter the discharge coefficient approaches a constant value.)

Although the discharge coefficient itself does not predict the data well because of the omission of vapor velocity effects, it does give some insight into the data and physical situation. The weir flowmeter calibration equations developed have the best accuracy in the free discharge region, which occurs above weir levels of 6.6 cm.

Also shown in Figure 16 are the relative uncertainties in the data. In the low flow clinging regime of the circled data of Figure 16, the uncertainty is higher at 10-14 percent. The uncertainty drops a modest amount in the transition regime where intermittence in the cling flow occurs. When the free discharge is established at 6.6 to 6.8 cm weir level, the flow becomes more stable, and the data uncertainty is seen to drop abruptly to 2 percent. This weir level is consistent with the discharge coefficient reaching a more consistent trend, and the low 2 percent data uncertainty is supportive of the calibration equations developed from these data.

In general, uncertainties for weir level, weir differential pressure and dewar pressure were estimated based on precision and bias errors from the instruments at 95% probability. The combined bias and precision error expressions for the flow rate were then found. A procedure for multiple-measurement uncertainty was applied to the data collected under fixed operating conditions[13].

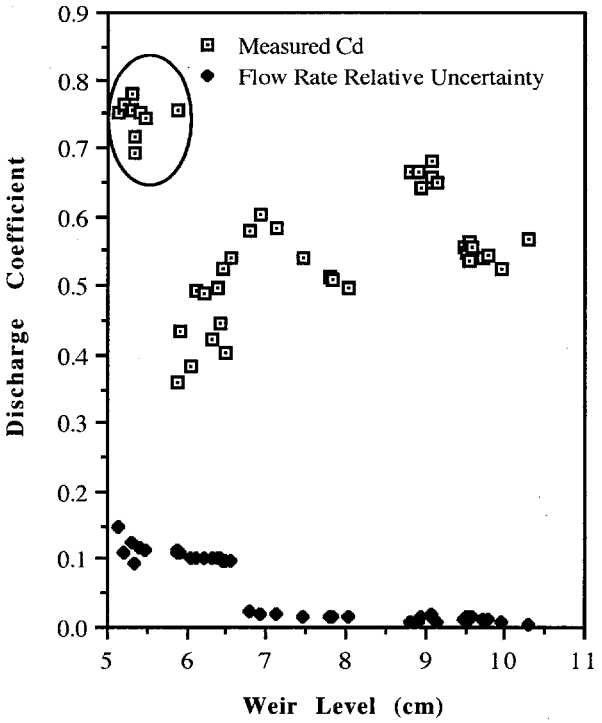

Figure 16 Discharge coefficient distribution and relative uncertainty of flow rate as a function of measured weir level.

Conclusions

The primary objective of this study was to develop a calibration equation for the liquid flow rate of saturated helium through a weir flowmeter. For this purpose, forty-five flow rate experiments were performed using the PS1 refrigeration system at Fermi National Laboratory.

In this enclosed weir, it was found that the vapor flow above affected the liquid flow rate over the weir. This factor was taken into account in predicting the flow rate via a differential pressure measurement across the weir.

Liquid flow rate calibration equations were developed from the data using different independent variables. Using all of the available variables, weir level, weir differential pressure, and system pressure, an accurate equation was developed Equation (13c) which predicted the higher flow, non-clinging data within an accuracy of ± 10%. This equation is recommended for obtaining the highest flow rate accuracy with the weir flowmeter.

Eliminating the system pressure as a secondary parameter, Equation (13b) was developed based on weir level and weir differential pressure. The prediction accuracy for non-clinging data was within ± 15%, and ± 20%, Equation (13d) was obtained using differential pressure alone. (This last result indirectly included weir level through the placement of the pressure taps.) These two equations produce reasonable prediction accuracy of flow rate, and they involve fewer measurements than the use of Equation (13c). These two equations are recommended where small prediction error can be traded against simplicity and reduced cost.

Acknowledgements

Thanks is extended to Robert Mau, Daniel Johnson, Paul Allcorn, Bryan Johnson and the operating crews of the Beams Division Operations Group at Fermilab for the assistance in monitoring some of the data test runs. Also, thanks to the staff members of the Beams Division Cryogenic Department, John Brubaker, Joel Fuerst, Arkadiy Klebaner, Alex Martinez, Barry Norris, Kenneth Olesen, William Soyars and Jay Theilacker. Thanks to Daniel Markley, William Noe Jr. and Richard Schmitt for their support regarding the Fixed DMACS control system and data recovery. Thanks to Thomas Peterson for his expert help with expansion engines.

References

[1] **Rao, L. N.** Theory of Weirs. *Advances in Hydroscience* 1975; 38: 309 – 329.

[2] **Peterson, Thomas J.** The Nature of the Helium Flow in Fermilab's Tevatron Dipole Magnets. *Cryogenics* 1997; 37: 11-19.

[3] **Theilacker, J.C. and Rode, C. H.** An Investigation Into Flow Regimes for Two-Phase Helium Flow. *Adv Cryog Eng* 1987; 33: 1748-1755.

[4] **Kuchnir, M.** Pressure Drop of Single Phase and Two Phase Helium Flow. *Fermilab Technical Memo-703* 1976.

[5] **Weisend II, J.G.** Handbook of Cryogenic Engineering. *Taylor and Francis* 1998: 2-295.

[6] **Merritt, F.S.** Standard Handbook of Civil Engineerings. *McGraw-Hill Co.* 1983; New York: 21-17 - 21-79.

[7] **King, H.W. and Brater, E.F.** Handbook of Hydraulics. *McGraw-Hill Book Co.* 1963; New York: 4-38 - 5-25.

[8] **Fox, R. W., McDonald, A.T.** Introduction To Fluid Mechanics. *John Wiley and Sons* 1985; New York: 546-552.

[9] **Urquhart, L.C.** Civil Engineering Handbook. *McGraw-Hill Book Co.* 1962; New York: 4-45 - 4-62.

[10] **Sanders, R. C., Rabehl, R. J. and McGee, M.W.** Weir Flow Meter for Saturated Liquid Helium. *Adv Cryog Eng* 1995; 41B: 1797 – 1802.

[11] **Efferson, K. R.** A Superconducting (Nb-Ti) Liquid Helium Level Detector. *Adv Cryog Eng* 1969; 15: 124-131.

[12] **Lenz, A. T.** Viscosity and Surface Tension Effects on V-Notch Weir Coefficients. *American Society of Civil Engineers* 1941: 759-801.

[13] **Figliola, R. S. and D. E. Beasley** Theory and Design for Mechanical Measurements. *Wiley and Sons* 1991: 143-239.